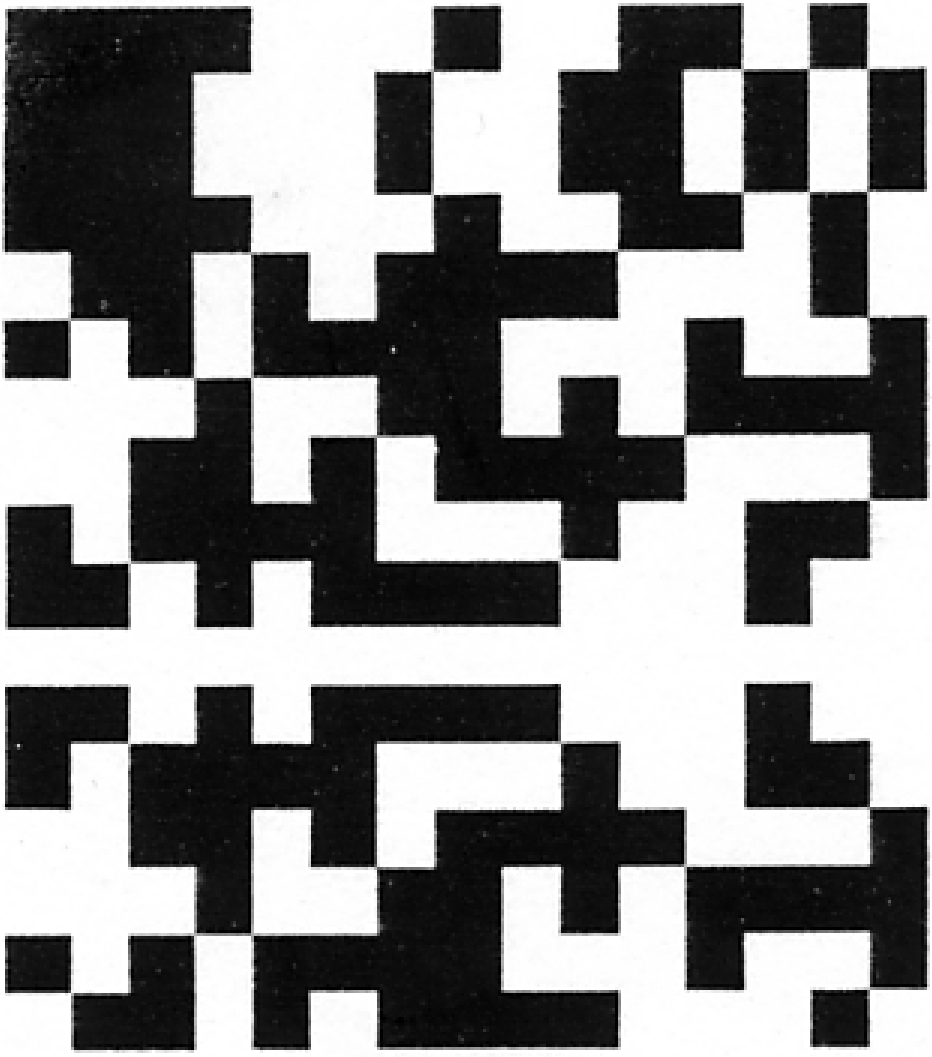

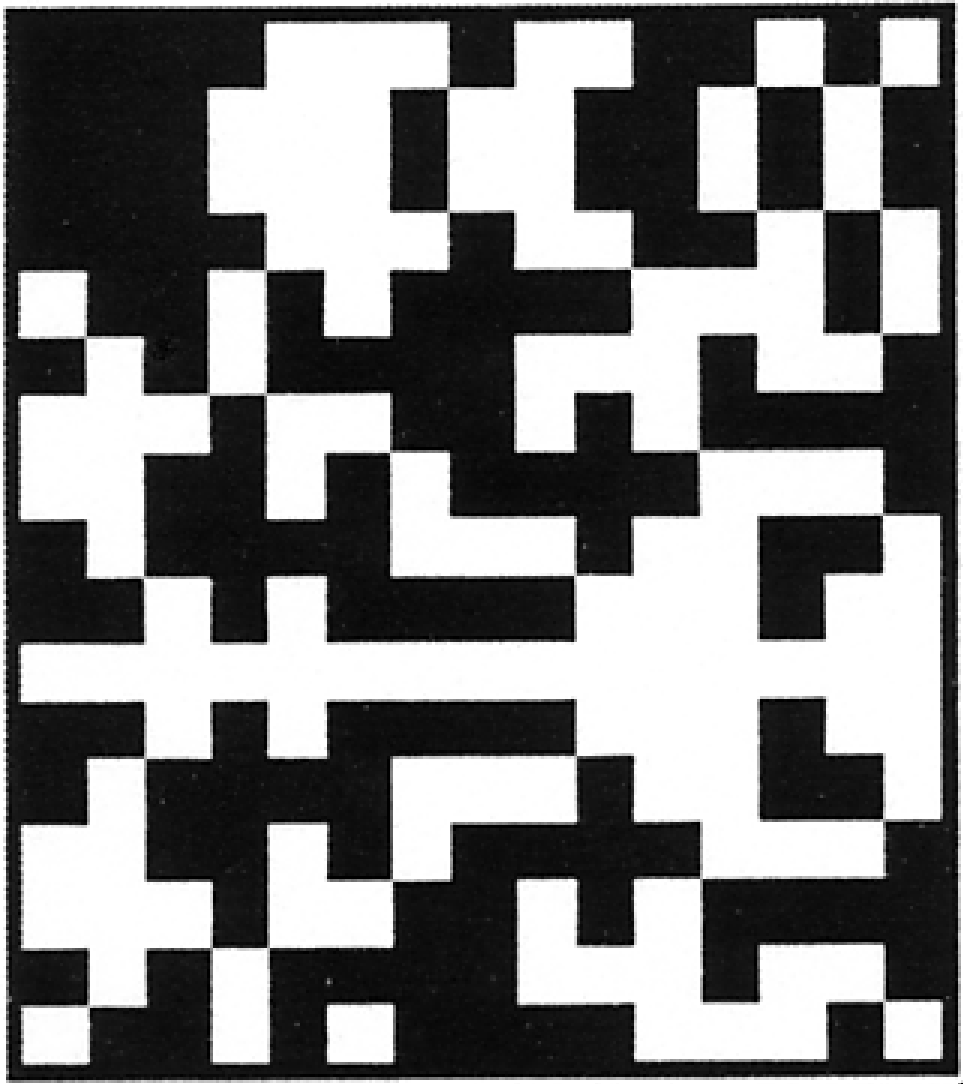

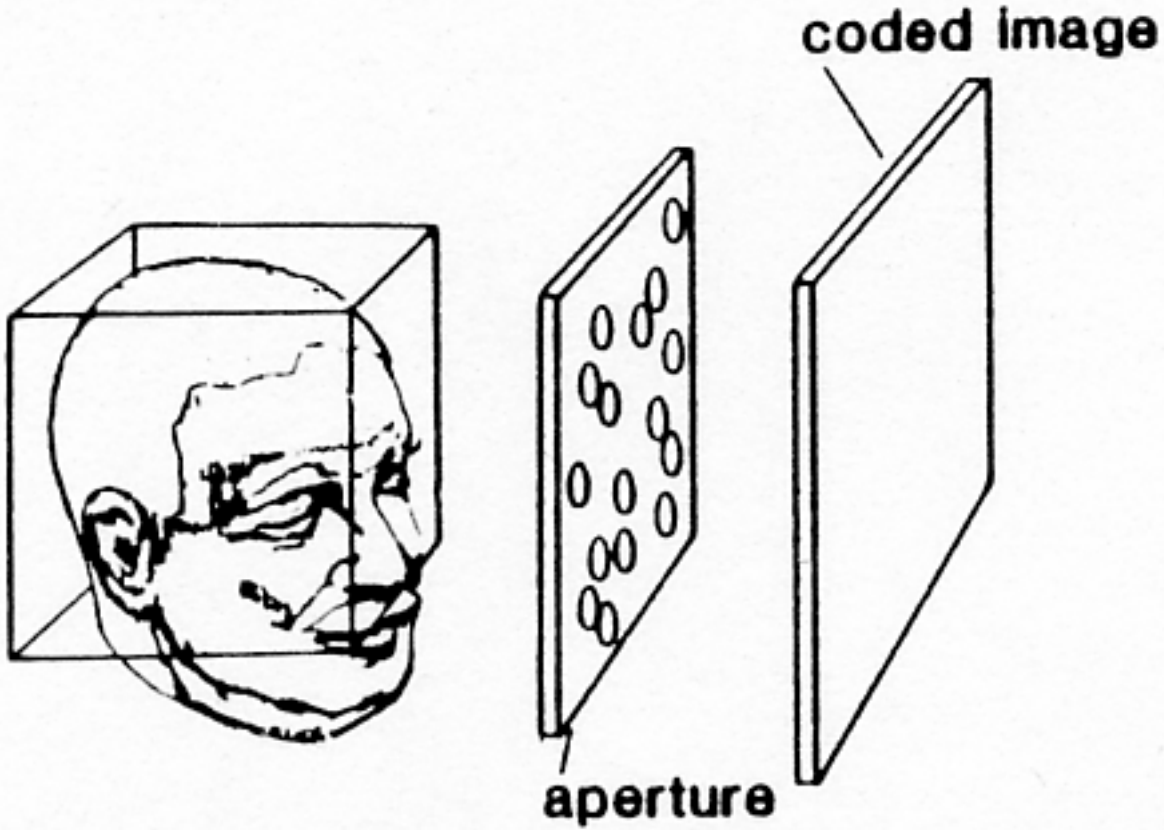

Fig. 1. Three-dimensional coded-aperture system incorporating a single view.

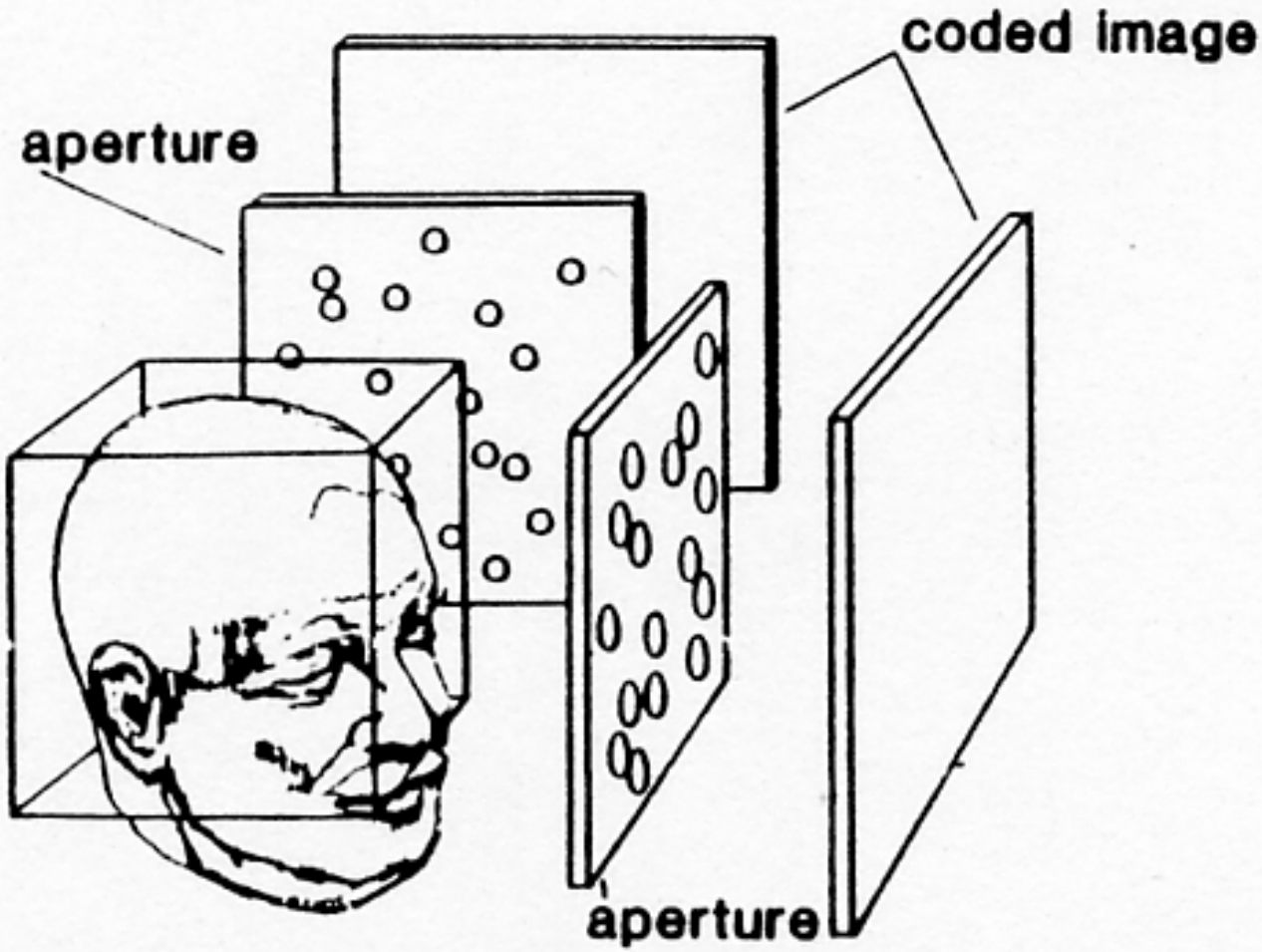

Fig. 2. Three-dimensional coded-aperture system incorporating orthogonal views.

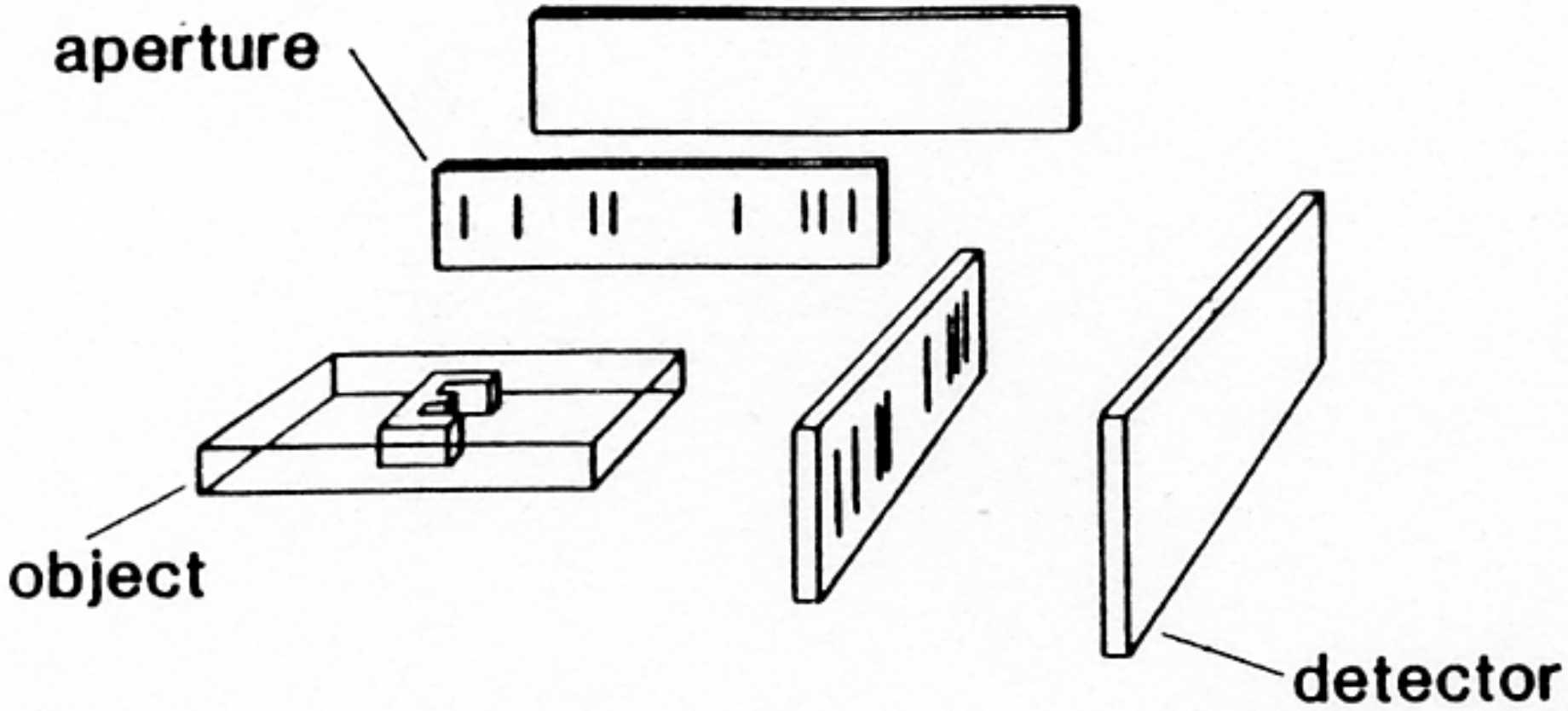

Fig. 1. Orthogonal-view coded-aperture system for two-dimensional object.

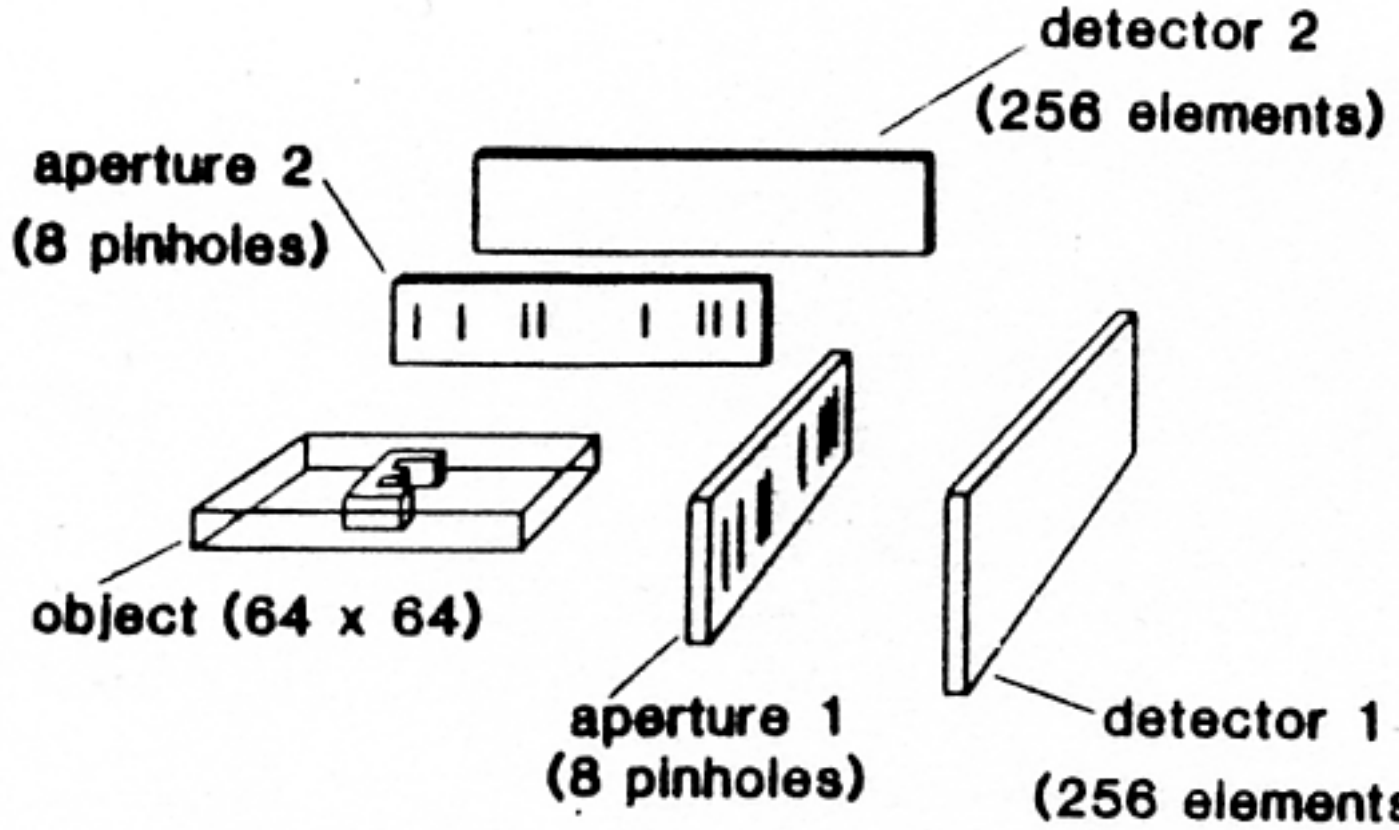

Fig. 3. Two-dimensional system with one-dimensional coded apertures. Each aperture is a uniformly redundant array of eight pinholes. If the object is a square of side 1 unit, each aperture is 1.40 units long (the extreme pinhole separation) at a distance of 0.95 unit from the square center, and each detector is 3.10 units long at a distance of 1.55 units from the square center.

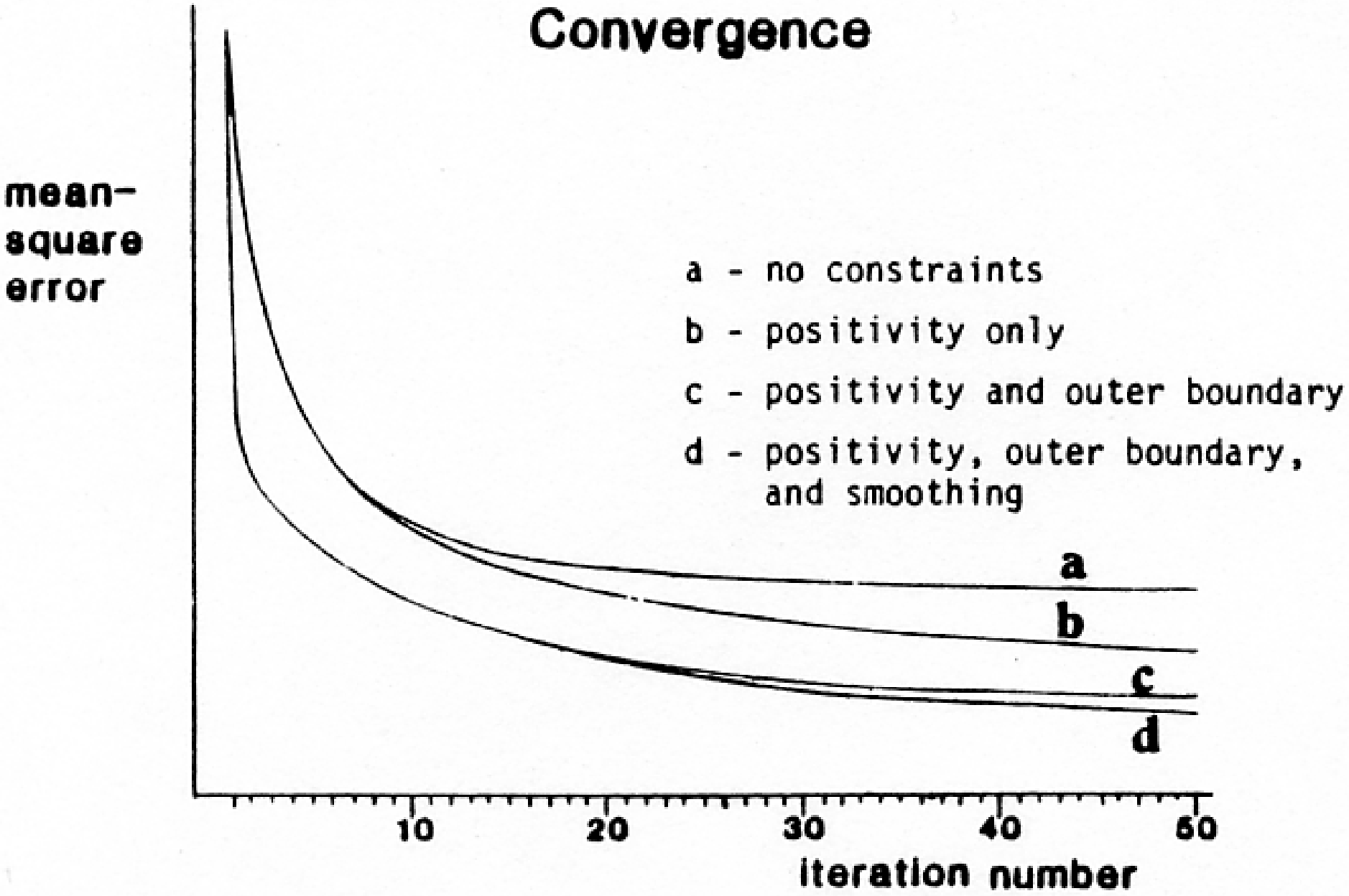

Fig. 8. Graph of the mean-square error of the reconstruction (formed using the iterative backprojection algorithm) versus iteration number for reconstructions using different constraints.

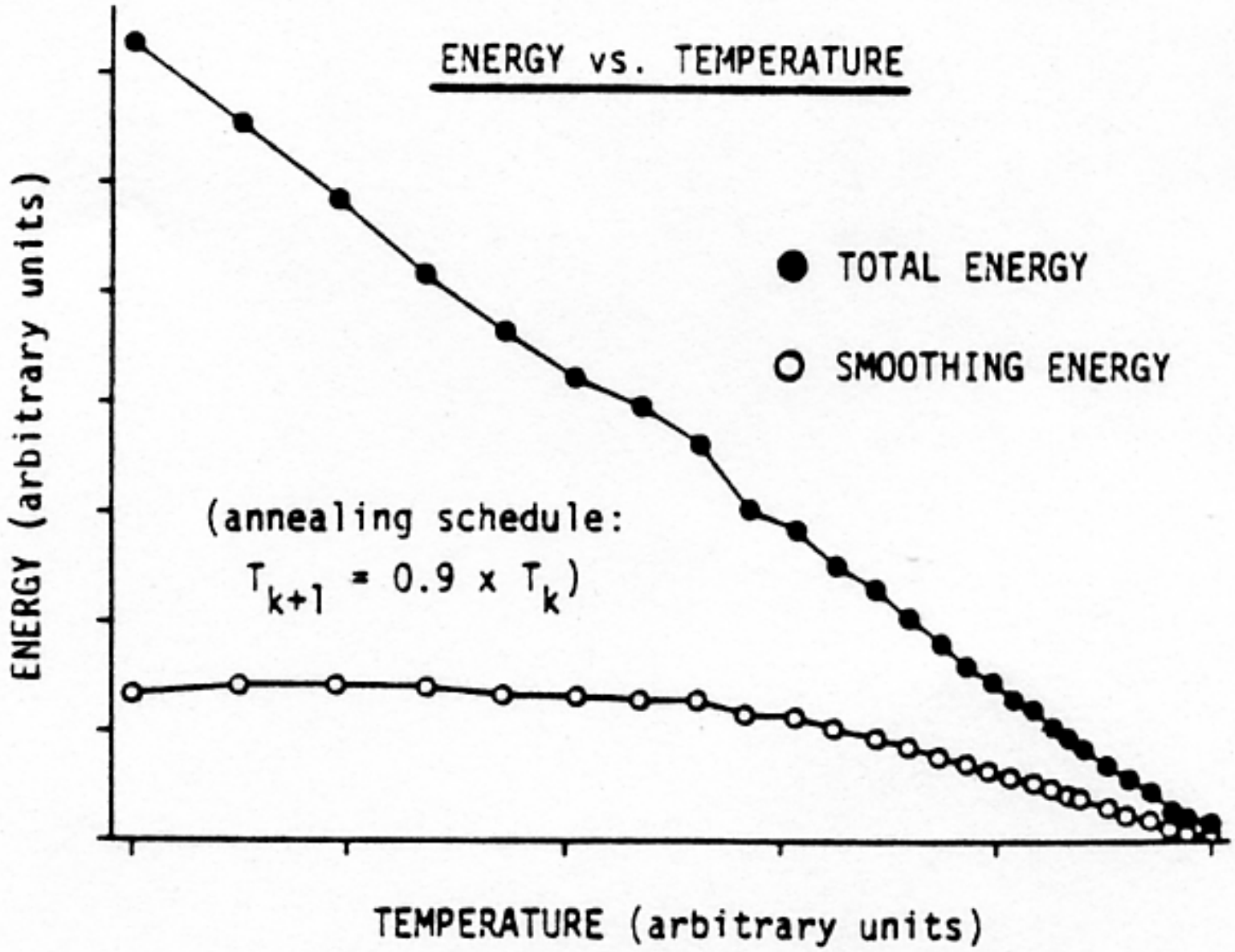

Fig. 11. Total energy (smoothing energy plus coded-image energy) and the smoothing energy versus the temperature for the 90% annealing schedule. Each data point is the average of three runs.

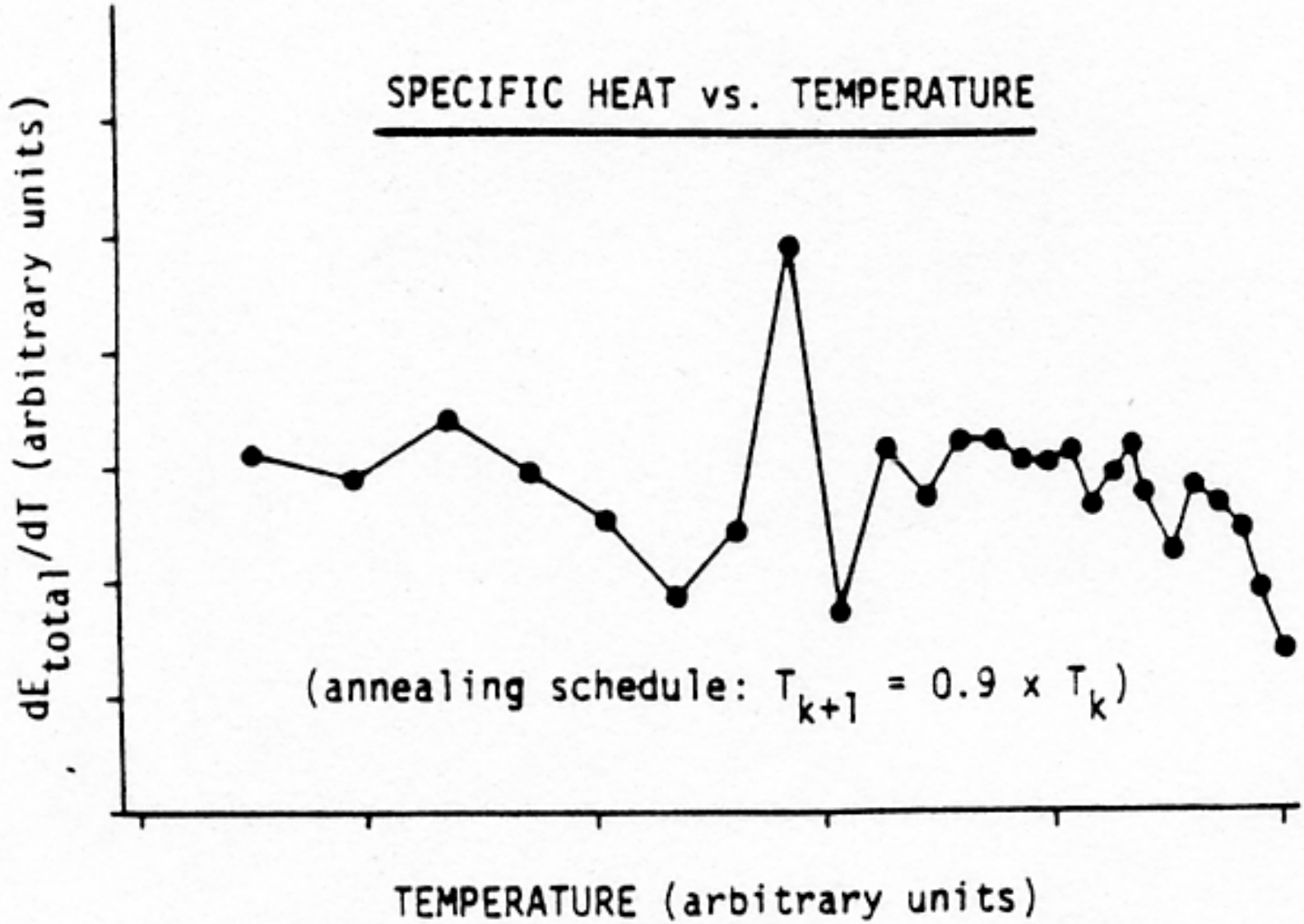

Fig. 12. The quantity $dE(\text{total})/dT$ (the specific heat) versus the temperature T, derived from Fig. 11.